Second-harmonic generation in a bent-core nematic liquid crystal

S. H. Hong,[1] J. C. Williams,[2] R. J. Twieg,[2] A. Jákli,[3] J. Gleeson,[1] S. Sprunt,[1] and Brett Ellman[1]
[1]*Department of Physics, Kent State University, Kent, Ohio 44242, USA*
[2]*Department of Chemistry, Kent State University, Kent, Ohio 44242, USA*
[3]*Chemical Physics Interdisciplinary Program and Liquid Crystal Institute, Kent State University, Kent, Ohio 44242, USA*
(Received 24 June 2009; revised manuscript received 3 March 2010; published 25 October 2010)

Second-harmonic generation (SHG) is studied in the magnetically aligned nematic phase of a bent-core liquid crystal (BCN) and compared to similar measurements made on a conventional rodlike (calamitic) nematic compound. The second-harmonic (SH) light detected from both materials is predominantly due to scattering and therefore incoherent. Results on the calamitic are consistent with a polarization induced by ordinary director fluctuations in the nematic phase. However, the SH scattering collected in the BCN exhibits a different temperature and angular dependence. We discuss how these differences could arise from the effects of short-range correlated, smectic-C—type molecular clusters, which have been detected in recent studies on various BCN materials.

DOI: 10.1103/PhysRevE.82.041710 PACS number(s): 61.30.−v, 72.80.Le

I. INTRODUCTION

Homogeneous, deformation-free nematic liquid crystals, whose orientational order is characterized purely by a symmetric, traceless second rank tensor order parameter, are centrosymmetric, and thus do not produce second-harmonic generation (SHG) arising from dipolar matrix elements. However, surface interactions, or bulk elastic distortions that induce a polarization through the flexoelectric effect [1], can break this symmetry. The effects of the former have been studied by SHG in thin layers of conventional calamitic (rod-shaped) nematics in contact with various solid surfaces [2], while the latter has been observed in bulk calamitic nematics containing static distortions of the optic axis (director) [3] or exhibiting strong thermal fluctuations of the director [4]. Recently, nematics formed from bent-core molecules (BCNs) have generated high interest, from the fundamental point of view, through reports of nematic biaxiality [5–7] and theoretical conjectures of entirely new phases, including a polar nematic [8]. On the practical side, certain BCNs exhibit a low-frequency flexoelectric effect [10] orders of magnitude larger than their calamitic counterparts, and may therefore eventually prove to be useful materials for small-scale, green power generation. These properties imply that SHG could be a revealing probe of BCN structure.

Here we present results of SHG experiments on a homogeneously aligned BCN (4-chloro-1,3-phenylene bis-4-[4′-(9-decenyloxy)benzoyloxy] benzoate, abbreviated ClPbis10BB [9]), and compare them to the behavior observed in a conventional calamitic nematic compound (4-n-octyl-4-cyanobiphenyl or 8CB). Our findings are twofold. First, for 8CB, we present data that confirm key and previously untested predictions of the model of incoherent nonlinear scattering induced by collective fluctuations of the optic axis, which was introduced and first applied by Copic and Ovsenik [4]. Second, in a BCN compound previously found to exhibit large flexoelectric response [10] in addition to other unusual properties [11,12], we observe that while the SH light also comes overwhelmingly from scattering, it has features notably different from the calamitic nematic. In particular, the SH signal in the BCN, while not unusually large, remains approximately constant in temperature (in contrast to the continuous decrease away from isotropic-nematic transition observed in 8CB). Additionally, the main contribution to the scattering is concentrated in a band or "halo" off the forward direction, whose angular dependence cannot be accounted for by nonlinear light scattering from ordinary director fluctuations. Instead, we suggest the additional component to the SH scattering in the BCN arises from the presence of short-range correlated, smectic-C-like molecular clusters, which have a polar layer structure. Evidence of these clusters has recently been detected in experiments on various BCNs [13,14], including the compound studied in this work [15].

II. EXPERIMENTAL DETAILS

Our experimental set-up and the structure of ClPbis10BB are shown in Fig. 1. ClPbis10BB exhibits the following phase sequence on cooling: isotropic–(76.1°)–uniaxial nematic–(65 °C)–crystal. Samples of ClPbis10BB and 8CB were loaded into commercial fused silica cuvettes with a 1 mm path length. The cuvettes were cleaned and dried according to the manufacturer's recommended procedures, and were used without any further surface treatment. The sample cells were inserted into a temperature-regulated oven with transparent fused silica windows. The temperature at the sample was controlled to better than 0.1 °C. To achieve uniform alignment of the nematic director on cooling from the isotropic to nematic phase, we used a commercial electromagnet (AlphaMagnetics, model 4600) equipped with tapered 50 mm pole faces. The insulated sample oven was carefully centered in a 25 mm gap between the pole faces. This arrangement produced a maximum applied magnetic field of 1.6 T at the sample. The field was oriented normal to the incident light and parallel to the cuvette faces. Samples were first warmed above the nematic-isotropic transition (temperature T_{NI}) and then slowly cooled with the field applied.

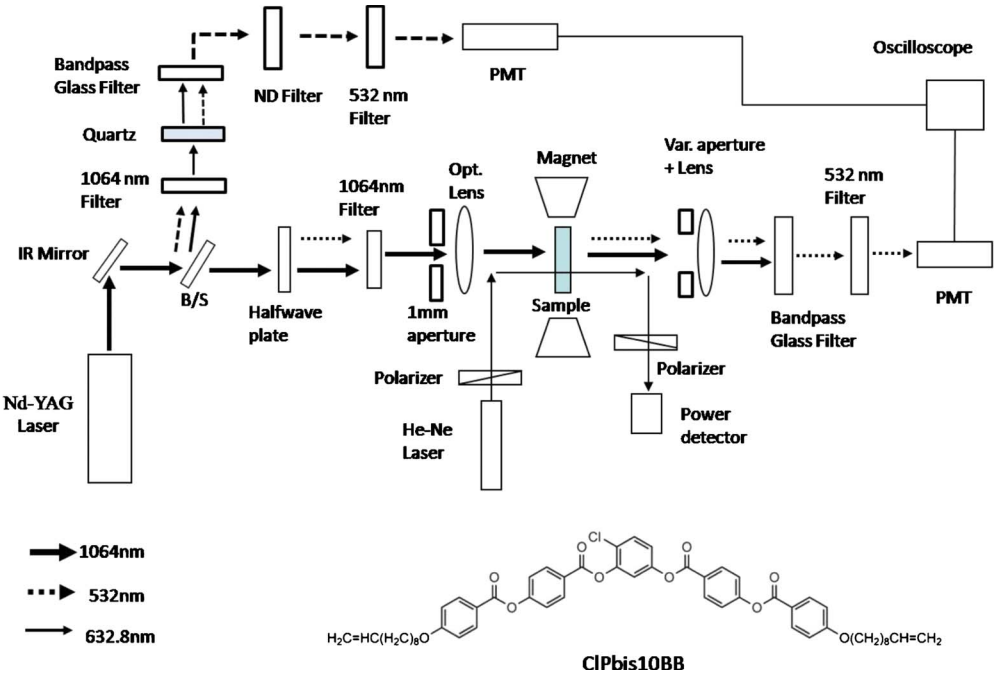

FIG. 1. (Color online) The experimental apparatus. Inset: The ClPbis10BB molecule.

To generate SH light, we used a Q-switched Nd:YAG laser (Continuum, Minilite series) with a wavelength of 1064 nm, producing a 3 mm diameter, linearly polarized Gaussian beam consisting of 5–7 ns pulses at a 10 Hz repetition rate. A half-wave plate was used to vary the incident polarization on the sample. An aperture was placed in front of the sample to reduce the beam size to ~1 mm, and for some measurements on the calamitic sample (8CB) a lens was used alternatively to focus the laser light to a ~0.4 mm waist at the sample. Typical average incident intensities were 7 MW/cm^2, corresponding to pulse energies of a few mJ for a 1 mm beam [16]. A low-pass optical filter was placed just before the sample to eliminate any 532 nm SH light generated by the incident optics. The forward transmitted SHG from the sample was collected and collimated by a 25 mm diameter fused silica lens with a 30 mm focal length. Immediately in front of the lens surface was a calibrated, variable iris, which was used to control the angular acceptance of the SHG light. The iris could be replaced with a 1 mm wide by 25 mm long slit, switchable between orientations along and perpendicular to the magnetic field direction. The collected light passed through a pair of Schott KG3 glass bandpass filters that efficiently block the 1064 nm fundamental, and then through a 532 nm narrowband (1 nm full width at half maximum) laser line filter, before finally passing onto a photomultiplier detector, which was placed about 0.5 m away from the magnet and shielded by multiple layers of mu-metal. During polarization scans, an analyzer was placed just before the 532 nm line filter.

The photocurrent output was converted to a voltage by a fixed terminating resistor and acquired by a digitizing oscilloscope (sampling rate=10 GHz). A snubbing cable was attached to the oscilloscope input to suppress ringing. Multiple (typically 100) pulses, read from the scope by computer, were area averaged; they were also normalized to the SHG signal from a 0.5 mm thick z-cut single crystal quartz reference plate. (The quartz reference signal was acquired on the incident side of our optical setup using a beam splitter, similar pre- and postoptical filtering as described above, a second photomultiplier, and an additional channel on the oscilloscope.) The weak background SHG from an empty cuvette placed in the oven was recorded and subtracted in all cases from the data obtained on the liquid crystal samples.

We also measured the depolarized transmittance of a HeNe laser beam through the samples, in order to independently confirm the isotropic to nematic phase transition temperature and to characterize the quality of director (optic axis) alignment in the nematic phase. A separate polarizer, analyzer, amplified photodiode detector, and flipper mirror assembly were used for these transmittance measurements.

III. RESULTS

We first focus on the optical transmittance measurements to confirm effective magnetic alignment of the nematic director. Figure 2 displays data for the transmission of a HeNe laser beam through a 1 mm thick sample of ClPbis10BB placed between crossed polarizers, as the polarizer/analyzer axes are simultaneously rotated through angle χ with respect to the magnetic field direction. These data were recorded after cooling the samples from the isotropic phase in the magnetic field to a temperature just below T_{NI}. We clearly see a well-defined minimum in transmission at $\chi=0$, corresponding to alignment of the polarizer (or analyzer) axes along the magnetic field direction; similar behavior was observed for the 8CB sample. Since prior magnetic field-induced optical anisotropy measurements on ClPbis10BB, combined with observation of a splay Freedericz transition in a homogeneously aligned planar sample, indicate positive diamagnetic anisotropy $\Delta\chi_m$ (which is also true for 8CB),

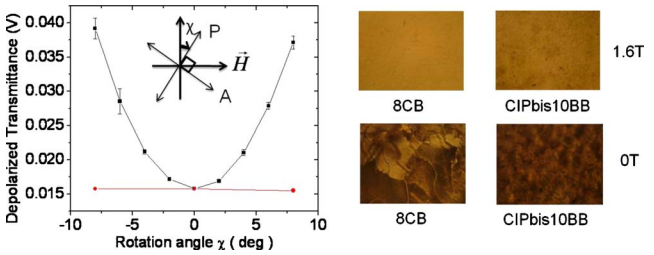

FIG. 2. (Color online) (Left) The depolarized transmittance of HeNe laser light through the magnetically aligned 1 mm ClPbis10BB sample as a function of polarizer angle with respect to the magnetic field direction, at the temperature $T-T_{NI}=-2.0$ °C in the nematic phase (squares) and at a typical temperature in the isotropic phase (circles). (Right) Bright-field optical textures of the 1.6 T field-aligned 8CB and ClPbis10BB samples, compared to unaligned samples (no applied field during cooling), in the nematic phase.

this result confirms good uniaxial alignment of the director along the field $\vec{H}$. We also note the optical clarity and uniformity in the bright-field microscope textures for field-aligned samples; these images were obtained *in situ* and are shown in Fig. 2. (For comparison, the figure includes textures for unaligned samples cooled from the isotropic state in zero field.)

Results for the temperature dependence of the SH light collected from field-aligned 1 mm nematic samples are presented in Fig. 3. For these measurements, the 1064 nm light was polarized at 45° to $\vec{n}$, yielding equal components of *o* and *e* polarized incident light. The analyzer was removed, and the collection aperture was adjusted to admit a cone of SH light with an acceptance angle of 20° into the detector. Starting from a temperature ~0.3 °C above the clearing point, the samples were cooled in fixed 0.1 °C steps at a

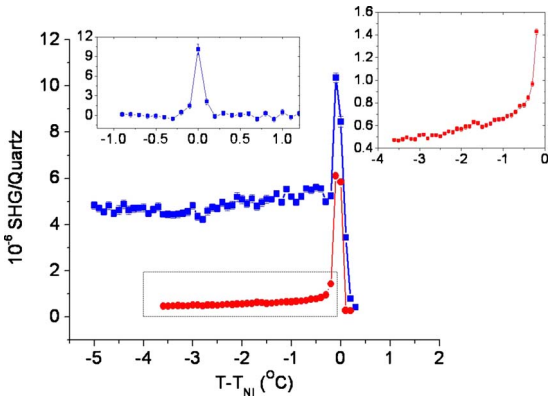

FIG. 3. (Color online) SHG power as a function of temperature for magnetically aligned, 1 mm thick samples of 8CB (lower data set, shown with filled circles) and ClPbis10BB (upper set, shown with squares), and for equal components of *o* and *e* polarization of the incident light and no analyzer for the SH light. The SH light is collected in a cone aound the forward direction as described in the text. Left inset: SHG power collected from a thin (10 μm) sample of ClPbis10BB. Right inset: detail of the boxed data for 8CB below T_{NI} from the main figure. (The weak background signal from empty sample cells has been subtracted in all cases.)

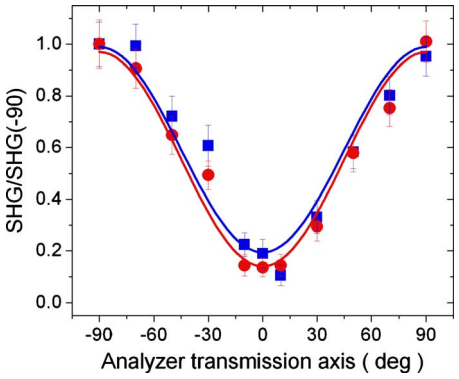

FIG. 4. (Color online) Normalized SHG power collected from the aligned nematic ClPbis10BB as a function of analyzer angle χ for *oo* (squares) and *ee* (circles) incident photons at a temperature $T-T_{NI}=-1.5$ °C. Solid lines are fits to a $\sin^2\chi$ dependence.

very slow rate (0.1 °C/h) between steps to ensure fully developed alignment (particularly in the bent-core case, where the orientational viscosities are quite high [11,12]). The SH power was recorded for each temperature step. At the end of the cooling scan, we reheated the samples and confirmed reproducibility of the data. In the case of 8CB, a few degrees into the aligned nematic phase, the SH power is of order 10^{-7} that recorded from the quartz reference and not much above the background level in the isotropic phase. As the inset shows, the signal increases by a factor of 2–3 as $T\rightarrow T_{NI}$ from the low temperature side. By contrast, in the BCN compound the SH power recorded below T_{NI} is approximately constant in temperature, and is substantially above the isotropic background level. For comparison, the SH signal at $T-T_{NI}=-1.5$ °C in ClPbis10BB is about 12 times the value at the same relative temperature in 8CB.

Figure 3 also shows data for SH power collected from a 10 μm thick sample of ClPbis10BB, which was prepared using same fused quartz substrates as the cuvette containing the thick sample. If the SH light collected is due primarily to scattering (as we shall discuss below—see Fig. 5), and is therefore incoherent, one expects the signal to scale with the number of scatterers and therefore with the illuminated path length. Away from the narrow transition region, the power collected from the 10 μm sample (100 times thinner than the 1 mm sample) is basically at the background level. (A similar result was confirmed for a thin layer of 8CB.) This reduction in signal with sample thickness is consistent with incoherent SHG, and thus also indicates that essentially none of the signal observed in the 1 mm sample below T_{NI} can be attributed to SH light generated from interfacial layers at the cell surfaces.

In Fig. 4 we show the variation of the SH light intensity from ClPbis10BB as a function of analyzer angle for pure ordinary (*o*) and extraordinary (*e*) incident polarizations and at $T-T_{NI}=-1.5$ °C. (The data are normalized to the value at the −90° analyzer setting.) The plots reveal a high contrast between maxima (for $oo\rightarrow o$ and $ee\rightarrow o$ SH processes) and minima (corresponding to nearly zero signal for the $oo\rightarrow e$ and $ee\rightarrow e$ processes). Here $oo\rightarrow e$, for example, stands for SH light produced when two ordinary-polarized photons (frequency ω) generate an extraordinary-polarized 2ω pho-

TABLE I. Summary of experimental results for dependence of the SH power on polarization and scattering vector orientation (with q_z parallel to the aligned director $\vec{n}$). The top entries apply for four polarization combinations of the incident and SH light and for scattering collected with the collection aperture fully opened. The bottom entry was obtained using the narrow slit as described in Sec. II of the text, and for equal combination of *o* and *e* incident light and no analyzer for the SH light.

	8CB	ClPbis10BB
Relative SH power	$T-T_{NI}=-0.3$ °C	$T-T_{NI}=-1.5$ °C
$P^{(2)}(ee\rightarrow o)/P^{(2)}(oo\rightarrow o)$	1.3	1.1
$P^{(2)}(oo\rightarrow o)/P^{(2)}(oo\rightarrow e)$	8.0	6.1
$P^{(2)}(ee\rightarrow o)/P^{(2)}(ee\rightarrow e)$	10	7.5
$P^{(2)}(q\simeq q_z)/P^{(2)}(q\simeq q_\perp)$	6.4	4.7

ton. The solid lines represent fits to a $\sin^2\chi$ dependence, where χ is the angle between the analyzer axis and the direction of the field $\vec{H}$. The polarization data, which are summarized in Table I, clearly establish that the SH light collected from ClPbis10BB is predominantly of ordinary polarization. Similar results were obtained for 8CB just below T_{NI}; these agree with the earlier study on 8CB reported in Ref. [4].

Utilizing the variable iris (radius R) or the narrow slit described in Sec. II, we probed the angular dependence of the scattered SH light. The iris or slit were placed just in front of the collimating lens and at a distance $L=30$ mm) from the illuminated sample volume. The top panel of Fig. 5 presents the SH signal detected as a function of $(R/L)^2=\tan^2\theta$ (θ=scattering angle) for normally incident, 45° polarized 1064 nm light and for both the aligned calamitic and BCN liquid crystals at several temperatures just below T_{NI}. These data were taken with the same cooling rate between temperature steps as the data in Fig. 3. For both samples, the collected SH signal is very small for R comparable to the

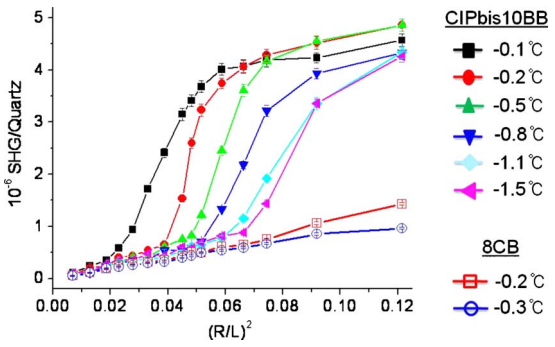

FIG. 5. (Color online) SH power $P^{(2)}$ collected from aligned samples of 8CB (open symbols in the lower part of the graph) and ClPbis10BB (filled symbols) plotted as a function of $\tan^2\theta=(R/L)^2$, where R is the collection aperture radius, L is the fixed aperture to sample distance, and θ is the scattering angle, at various temperatures (given as $T-T_{NI}$) in the nematic phase. Equal *o* and *e* components of incident (1064 nm) light polarization were used, with no analyzer for the SH light.

incident beam diameter—i.e., for SH light propagating along the direction of the fundamental beam—and increases monotonically with R for SH light scattered off this direction. The results thus show that scattering dominates the signal. However, the nature of the scaling of the collected SH power ($P^{(2)}$) with R is clearly quite different between the calamitic and BCN. For the former, in the narrow range just below T_{NI} where the signal level was sufficient to allow detailed measurements, we observe that $P^{(2)}$ is essentially proportional to collection area, $P^{(2)}\propto R^2$. On the other hand, the data for ClPbis10BB reveal that, apparently superimposed on a weaker R^2 dependence, is a more rapidly increasing contribution that dominates $P^{(2)}$ at the larger values of R or angle θ. This component clearly contributes away from the forward direction, and is therefore consistent with a band (or halo) of scattering surrounding a node (or minimum) in the forward direction. The band evidently shifts to higher θ with decreasing temperature.

To complete our summary of the main experimental results, we consider the directional dependence of the scattered SH light for equal *o* and *e* components of normally incident fundamental light. As recorded in Table I, data for orientations of the collection slit along or perpendicular to $\vec{n}$ reveal that the SH light for both 8CB and ClPbis10BB is predominantly scattered in directions parallel to $\vec{n}$. A similar result was found for all temperatures studied in the nematic phase.

IV. DISCUSSION

The SH signal in our experiments is only of order $\sim 10^{-6}$ the level from the quartz reference plate. It is therefore prudent to consider first the contribution expected from single molecule hyper-Rayleigh scattering (SMHRS), which corresponds to incoherent scattering at 2ω from thermodynamic fluctuations in *individual* molecular configurations. As has been pointed out in Ref. [4], the signal due to SMHRS should change by only a factor of order unity at the isotropic-nematic transition; on the other hand, our observed signals in the nematic phase—near T_{NI} in the calamitic sample and throughout the nematic range in the BCN—are definitely above the isotropic level. We can also estimate the magnitude of the SMHRS signal that could be present in our experiments. One can write [17,18] $I(2\omega)=GN\langle\beta^2\rangle I(\omega)^2$ for the intensity of the second-harmonic light, where G is a geometric factor for dipole scattering ($G=2048\pi^5/c\lambda^4r^2$, λ=fundamental wavelength, r=distance from illuminated volume of the sample to the aperture collecting the SH light), N is the number of molecules exposed to incident light of intensity $I(\omega)$, and $\beta^2=\Sigma_{ijk}\beta_{ijk}\beta_{ijk}$ with the tensor β being the single molecule hyperpolarizability. The average $\langle\rangle$ is taken over the appropriate distribution of molecular orientations, and cgs units for electric charge are assumed in the definition of G. While we do not know β precisely for our LC molecules, standard density functional theory calculations of geometrically optimized structures (using the B3LYP functional and 6-31g* basis set [19]) provide maximum components of hyperpolarizability of order 20×10^{-30} cm^5/statC, which is the same order of magnitude as deduced from recent measurements on bent-core liquid

crystals dissolved in suitable solvents [20]. With this value for β, the known beam waist, laser energy per pulse, sample thickness, sample to collection aperture distance, aperture radius, and the molecular weight and density of ClPbis10BB, we estimate a maximum signal from SMHRS of a few photons per pulse, which is within the level measured in the isotropic phase. Based on the above considerations, we rule out SMHRS as a significant contributor to the SH scattering observed in the nematic phase of our samples.

Let us now turn to sources of SH light involving intermolecular interactions and collective effects. For these sources, the induced SH polarization may be written as [21–23]

$$\vec{P}^{(2)} = \overleftrightarrow{\chi}^{(2)}:\vec{E}\vec{E} + \overleftrightarrow{\chi}_Q^{(2)} \vdots \vec{E}\vec{\nabla}\vec{E} + \overleftrightarrow{\chi}^{(3)} \vdots \vec{E}_P\vec{E}\vec{E} + \overleftrightarrow{\chi}_S^{(2)}:\vec{E}\vec{E}\delta[r' - h(r')] \quad (1)$$

where each term is evaluated at point $\vec{r}'$ in the sample and $\vec{E}$ is the fundamental optical field. The first term in Eq. (1)represents a bulk structural (equilibrium) noncentrosymmetry; it vanishes in a homogeneous uniaxial nematic liquid crystal. The second arises from nonlocal ("quadrupolar") interactions in the bulk, and is permitted in centrosymmetric media such as ordinary nematics. The third term describes an SH polarization through a third order combination of a zero-frequency electric field ($\vec{E}_P$), which perturbs the medium from its equilibrium state, and two optical fields; it is also allowed in centrosymmetric media. The final term accounts for surface noncentrosymmetry, which may arise in heterogeneous media or at the sample boundaries; the function $h(r')$ specifies the relevant surfaces.

In the Rayleigh Debye Gans (RDG) approximation, the fundamental field at any source point $\vec{r}'$ in the medium is assumed to have the form of the incident plane wave,

$$\vec{E}(\vec{r}',t) = E_0\hat{\pi}\exp i(\vec{k}\cdot\vec{r}' - \omega t) \quad (2)$$

where $\hat{\pi}$ specifies the polarization direction in the sample, and $\vec{k}=n(\omega)(\omega/c)\hat{k}$. Under this assumption, and in the far-field approximation, the second order nonlinear radiation field at point $\vec{r}$ on the detection aperture is given by

$$\vec{E}^{(2)}(\vec{r},t) = \frac{\omega^2 \exp[i2\omega(r-ct)/c]}{\pi\epsilon_0 c^2 r}[\vec{p}_{eff}^{(2)} - \hat{k}^{(2)}(\vec{p}_{eff}^{(2)}\cdot\hat{k}^{(2)})] \quad (3)$$

Here r is the distance from source to detector (directed along $\hat{k}^{(2)}$), conventional (SI) units for charge and the speed of light $\nu\cong c$ are assumed. The effective nonlinear dipole moment $\vec{p}_{eff}^{(2)}$ is obtained from Eq. (1) as [23]

$$\vec{p}_{eff}^{(2)} = E_0^2\int dV'[\overleftrightarrow{\chi}^{(2)}:\hat{\pi}\hat{\pi} + i\overleftrightarrow{\chi}_Q^{(2)} \vdots \hat{\pi}\vec{k}\hat{\pi} + \overleftrightarrow{\chi}^{(3)} \vdots \vec{E}_P\hat{\pi}\hat{\pi} + \overleftrightarrow{\chi}_S^{(2)}:\hat{\pi}\hat{\pi}\delta(r' - h(r'))]\exp[i(2\vec{k} - \vec{k}^{(2)})\cdot\vec{r}'] \quad (4)$$

with $\vec{k}^{(2)}=n(2\omega)(2\omega/c)\hat{k}^{(2)}$. The integral is taken over the illuminated volume of the sample. The average SH intensity at the detector, assuming no analyzer, is

$$I^{(2)} = \frac{1}{2}c\epsilon_0\langle\vec{E}^{(2)*}\cdot\vec{E}^{(2)}\rangle = \frac{\omega^4}{2\pi^2\epsilon_0 c^3 r^2}[\langle|\vec{p}_{eff}^{(2)}|^2\rangle - \langle(\vec{p}_{eff}^{(2)}\cdot\hat{k}^{(2)})^2\rangle], \quad (5)$$

where the angled brackets denote a statistical average over fluctuating quantities that may contribute to $\vec{p}_{eff}^{(2)}$. When an analyzer ($\hat{\pi}^{(2)}$) is present, the appropriate expression for $I^{(2)}$ can be calculated using the transmitted component of $\vec{E}^{(2)}$, or $\hat{\pi}^{(2)}\cdot\vec{E}^{(2)}$.

A. Uniaxial calamitic nematic (8CB)

Since $\overleftrightarrow{\chi}^{(2)}=0$ in the bulk of a uniaxial nematic, and since our comparison of results in thick and thin cells indicates no significant SH signal coming from the cell surfaces, for our analysis of data on the conventional calamitic (8CB) we consider the contributions from the second and third terms in Eq. (1) only. Let us first focus on $\overleftrightarrow{\chi}_Q^{(2)}$. An expression for this tensor has been derived by Zhong-can *et al.* [24], based on an application of the theory of SHG in lossless dielectrics developed by Bloembergen *et al.* [25] to a uniaxial nematic with $D_{\infty h}$ symmetry. The result is

$$\chi_{Q,ijkl} = \chi_1(n_i n_j\delta_{kl} - n_i n_k\delta_{jl} + n_k n_l\delta_{ij} - n_j n_l\delta_{ik}) + \chi_2(\delta_{ij}\delta_{kl} - \delta_{ik}\delta_{jl}),$$

where χ_1, χ_2 are material constants and $\vec{n}$ is the uniaxial director. One can show that, for both the uniform and fluctuating parts (the latter obtained with the substitution $\vec{n}\rightarrow\vec{n}_0+\delta\vec{n}$ where $\vec{n}_0\cdot\delta\vec{n}=0$), the SH intensity due to $\overleftrightarrow{\chi}_Q^{(2)}$ vanishes for the dominant processes $oo\rightarrow o$ and $ee\rightarrow o$ detected experimentally. (For the fluctuating part and the case $ee\rightarrow o$ only, the result follows specifically for normal incidence, $\vec{k}\cdot\vec{n}_0=0$, the condition we used in our experiment.)

Thus we are left with the term $\overleftrightarrow{\chi}^{(3)} \vdots \vec{E}_P\vec{E}\vec{E}$ in Eq. (1) to account for the SH signal detected. In fact, this term can be related to a model previously developed and applied by Copic and Ovsenik (CO) [4] to describe fluctuation-induced SH scattering in nematics. Their theory is physically based on coupling of the director modes to the flexoelectric polarization—i.e., the polarization induced by curvature strains in $\vec{n}$—which is a well known, though typically weak, phenomenon in ordinary nematics [26]. We shall show that a version of the CO approach, based on a $\overleftrightarrow{\chi}^{(3)}$ process (allowed in centrosymmetric media such as uniaxial nematics), provides a good account of our data on 8CB, but at the same time does not adequately explain important features observed in our BCN sample.

For our development of the model, we treat the flexoelectric polarization $\vec{P}_{flex}$, arising from overdamped thermal fluctuations of $\vec{n}$, as the source of a quasi-dc field that combines with the optical field of the fundamental light to generate SH scattering. To lowest order, we neglect the dielectric anisotropy and write $\vec{E}_P=\vec{P}_{flex}/\epsilon_0\bar{\chi}_e$, where $\bar{\chi}_e$ is the average dielectric susceptibility and $\vec{P}^{flex}$ takes the standard form [26],

$$P_j^{flex} = e_1 n_j\partial_m n_m + e_3 n_m\partial_m n_j, \quad (6)$$

Here e_1, e_3 represent material-dependent flexoelectric coefficients corresponding, respectively, to elastic splay and bend

distortions of the director $\vec{n}$, and the partial derivatives are abbreviated as $\partial_m = \partial/\partial x_m$. The third term in Eq. (4) now becomes

$$\vec{p}_{eff}^{(2)} = \frac{E_0^2}{\epsilon_0 \bar{\chi}_e} \int dV' \overleftrightarrow{\chi}^{(3)} \vdots \vec{P}_{flex} \hat{\pi}\hat{\pi} \exp[i(2\vec{k} - \vec{k}^{(2)}) \cdot \vec{r}']. \quad (7)$$

For a uniform nematic in equilibrium, the flexoelectric polarization in Eq. (6) will only contain a fluctuating part (δP^{flex}). The integrand in Eq. (7) is then proportional to $\chi^{(3)} \delta P^{flex}$. The $\chi^{(3)}$ tensor has an equilibrium part that has the symmetry of a uniaxial nematic, and a small fluctuating part $\delta\chi^{(3)}$, which we may ignore as it appears in the integrand as a product with the small quantity δP^{flex}. Thus, in calculating the contribution to $\vec{p}_{eff}^{(2)}$ that is linear in the nematic fluctuations, we will use the equilibrium $\chi^{(3)}$, and the fact that all components of this tensor with a non-recurring index vanish by the reflection symmetry of a uniaxial nematic [27].

Choosing z as the alignment axis along the field $\vec{H}$, we can write the director as a sum of uniform and small fluctuating parts, $\vec{n} = \hat{z} + \delta n_x \hat{x} + \delta n_y \hat{y}$. Then expressing $\delta\vec{n}$ in terms of its spatial Fourier transform, $\delta\vec{n}(\vec{r}',t) = V\Sigma_{\vec{q}} \delta\vec{n}(\vec{q},t) \exp(-i\vec{q}\cdot\vec{r}')$ [26], substituting into Eq. (6), and combining the result with Eq. (7), we obtain

$$\vec{p}_{eff}^{(2)} = -i \frac{E_0^2}{\epsilon_0 \bar{\chi}_e} [e_1 (\vec{q} \cdot \delta\vec{n}) \overleftrightarrow{\chi}^{(3)} \vdots \hat{z}\hat{\pi}\hat{\pi} + e_3 q_z \overleftrightarrow{\chi}^{(3)} \vdots \delta\vec{n}\hat{\pi}\hat{\pi}], \quad (8)$$

where $\delta\vec{n} = \delta\vec{n}(\vec{q},t)$ are Fourier components of the fluctuating part of the director at wave vector $\vec{q} = 2\vec{k} - \vec{k}^{(2)}$.

Next we substitute Eq. (8) into Eq. (5) to obtain the scattered SH intensity $I^{(2)}$. In order to calculate the resulting thermal averages over the director fluctuations, we express the fluctuations $\delta\vec{n}$ as a combination of the normal director modes—splay-bend (δn_1) and twist-bend (δn_2)—of a uniaxial nematic. Using the standard expressions for these modes, and for the elastic free energy of a uniaxial nematic, one obtains [26], $\langle \delta n_i^*(\vec{q},t) \delta n_j(\vec{q},t) \rangle = \delta_{ij} V k_B T / (K_i q_\perp^2 + K_3 q_z^2 + \Delta\chi_m H^2)$, where $i,j = 1,2$, $q_\perp^2 = q_x^2 + q_y^2$, $\Delta\chi_m$ is the diamagnetic susceptibility anisotropy, and K_1, K_2, K_3 are the elastic constants for splay, twist, and bend director distortions, respectively. In terms of explicit components of $\overleftrightarrow{\chi}^{(3)}$, Eqs. (8) and (5) then lead to

$$I^{(2)}(\vec{q}) = \frac{V E^4 k_B T \omega^4}{2\pi^2 r^2 \bar{\chi}_e^2 \epsilon_0^3 c^3} \sum_{n=1,2} \frac{\vec{X}_n \cdot \vec{X}_n - (\hat{k}^{(2)} \cdot \vec{X}_n)^2}{K_n q_\perp^2 + K_3 q_z^2 + \Delta\chi_m H^2}, \quad (9)$$

where

$$X_{1i} = \pi_k \pi_l \left[e_1 \chi_{izkl}^{(3)} q_\perp + e_3 \left(\chi_{ixkl}^{(3)} \frac{q_x}{q_\perp} + \chi_{iykl}^{(3)} \frac{q_y}{q_\perp} \right) q_z \right],$$

$$X_{2i} = \pi_k \pi_l e_3 \left(\chi_{iykl}^{(3)} \frac{q_x}{q_\perp} - \chi_{ixkl}^{(3)} \frac{q_y}{q_\perp} \right) q_z. \quad (10)$$

In these expressions, summation is implied on repeated indices. For the range of aperture opening angles over which a signal above background level is recorded in Fig. 5, and with typical values of K and $\Delta\chi_m$ in thermotropic nematics and $H = 1.6$ T, we estimate that the term $\Delta\chi_m H^2$ is negligible in the denominator of Eq. (9). Then taking x as the direction for ordinary polarization, y as the direction of normally incident (fundamental) light, and z as the extraordinary axis (as already assumed above), and using the symmetry of a uniaxial nematic, one finds from Eq. (10) that the following components of the $\chi^{(3)}$ tensor contribute for the ω, 2ω polarization combinations probed in our experiments:

$$\chi_{xxxx}^{(3)}, \chi_{yyxx}^{(3)} (oo \to o)$$

$$\chi_{xxzz}^{(3)}, \chi_{yyzz}^{(3)} (ee \to o)$$

$$\chi_{zzxx}^{(3)} (oo \to e), \chi_{zzzz}^{(3)} (ee \to e).$$

Let us now consider two limits of Eqs. (9) and (10) and apply these to our data for 8CB. First suppose $q = q_z$. As described in the Sec. II above, this case is picked out by orienting a thin collection slit along the field $\vec{H}$, and, as noted in Table I, it yields the overwhelming majority of the observed SH signal. Taking $q \simeq q_z$ in Eq. (10), one finds that the contributing elements of the $\chi^{(3)}$ tensor from the above list are $\chi_{xxxx}^{(3)}$, $\chi_{yyxx}^{(3)}$, $\chi_{xxzz}^{(3)}$, and $\chi_{yyzz}^{(3)}$. These are the components that correspond to the processes $oo \to o$ and $ee \to o$, which, also according to Table I, produce the most significant SH signal. On the other hand, the limit $q = q_\perp$ in Eqs. (10) applies for slit orientation normal to $\vec{H}$, which yields substantially smaller SH power in our experiment. This limit, in turn, contains the tensor components $\chi_{zzxx}^{(3)}$ and $\chi_{zzzz}^{(3)}$ corresponding to the polarization processes $oo \to e$ and $ee \to e$ that contribute very weak SH power in our experiment. Our data for 8CB combined with the fluctuational scattering model therefore suggest that $\frac{e_3^2}{K_3}[(\chi_{xxxx}^{(3)})^2 + (\chi_{yyxx}^{(3)})^2] \sim \frac{e_3^2}{K_3}[(\chi_{xxzz}^{(3)})^2 + (\chi_{yyzz}^{(3)})^2] \gg \frac{e_1^2}{K_1}(\chi_{zzxx}^{(3)})^2 \sim \frac{e_1^2}{K_1}(\chi_{zzzz}^{(3)})^2$. (In fact, the condition may be further simplified, since for fairly low scattering angles, such as used in our experiment, the terms in Eq. (10) containing the y component of the scattered polarization—i.e., the component parallel to the incident beam direction—will be weak.) Even without a direct confirmation of this condition based on measured values for the components of $\overleftrightarrow{\chi}^{(3)}$, we have still, significantly, confirmed the consistency between the polarization and $\vec{q}$-orientational dependences of the scattered SH light that is predicted by the theory.

The model also accounts for our finding that the SH power detected from the 8CB sample is linearly proportional to the area of the collection aperture (i.e., $P^{(2)} \propto R^2$ in Fig. 5). Under the condition on the relative magnitudes of the $\chi^{(3)}$ components mentioned above, and if we assume that the nematic elastic constants are equal to first order and that $\Delta\chi_m H^2$ is negligible (as noted previously), the leading angular dependence of Eq. (9) can be expressed in simple terms. Using coordinates θ, ϕ, where θ is the angle between a scattered SH ray and the incident direction of the fundamental light and ϕ is the angle describing the orientation of the SH ray in the plane perpendicular to the incident direction, we find $I^{(2)} \propto \cos^2(\theta/2) \sin^2\phi [1 + O(\sin^2\theta)]$. Neglecting the higher order term, whose maximum value is ~0.1 in our

experiment, we obtain the integrated SH intensity over the aperture of radius R as:

$$P^{(2)} = \int_{aperture} I^{(2)} dA \propto \int (R^2 + L^2)\cos^2(\theta/2)\sin\theta d\theta \int \sin^2\phi d\phi$$
$$= \frac{\pi}{2}(3 + \cos\theta)(R^2 + L^2)\sin^2(\theta/2),$$

where L is the distance from the sample to center of the aperture. For small values of $\theta/2$, one has $\sin^2(\theta/2) \approx \frac{1}{4}\sin^2\theta = R^2/4(R^2+L^2)$ and $\cos\theta \approx 1$, so that $P^{(2)} \propto R^2$ to lowest order, which accurately describes the data in Fig. 5 for 8CB [28]. This result basically stems from the fact that $I^{(2)}$ does not depend on the magnitude of $\vec{q}$, provided the term $\Delta\chi_m H^2$ in Eq. (9) is small, as noted previously by CO.

As a further point of comparison, we can use Eq. (9) to describe qualitatively the pretransitional temperature dependence of the SHG observed in 8CB that is evident from the inset to Fig. 3. According to the Landau–de Gennes phenomenological theory [26,29] (and also to experiments on standard calamitics [30]), the nematic elastic constants for splay and bend distortions may be expressed in terms of the scalar nematic order parameter S as $K_i = K_0 S^2 + K_i' S^3$ $(i=1,3)$. (Within the phenomenological theory, the second term is necessary to account for the anisotropy actually observed in the elastic constants.) For the flexoelectric coefficients, experiments on calamitic liquid crystals indicate $|e_1 - e_3| \sim S$ [31], so we take $e_i = e_{i0} S$. Because the third order susceptibility $\chi^{(3)}$ does not require nematic order for its existence, we treat its possible dependence on S, and thus its temperature dependence, as secondary factors. Equation (9) therefore predicts for the SH power, $P^{(2)} \propto e^2/K \sim e_{i0}^2/(K_0 + K_i' S)$. As $T \to T_{NI}$ from below, S decreases, and thus $P^{(2)}$ should increase, in agreement with the data for 8CB presented in Fig. 3.

B. Bent-core nematic (ClPbis10BB)

Now we turn to the distinctive behavior observed in the bent-core nematic sample. The correlation between SH polarization selectivity and $\vec{q}$-orientation is similar to 8CB (see Table I), and the fluctuation-based theory discussed above *could* explain the essentially constant level of the SH signal observed below the isotropic-nematic transition in the BCN compound if $e_i \sim S$ and the splay and bend elastic constants scaled strictly as S^2. However, the latter are known to be anisotropic in ClPbis10BB [32]; so at least within the widely applicable Landau–de Gennes theory for a uniaxial nematic, higher orders of S must appear in the elastic constants, and the scenario $e^2/K \sim S^2/S^2 \sim$ const is excluded. More significantly, as pointed out in Sec. III, the data for ClPbis10BB in Fig. 5 indicate that an excess band of SH light (whose power does not simply scale with collection aperture area) is scattered off the incident direction of the fundamental beam, and into an angular range that varies with temperature just below T_{NI}. In fact, the enhanced level of SH signal recorded from the BCN with a fully open aperture (Fig. 3) can be attributed to this halo, which is not present in the data on the calamitic sample. It is evident that we should consider an additional source for SH scattering to understand the results on the BCN.

Recent small angle Xray scattering (SAXS) measurements on various BCNs [13,14], including our own experiments on ClPbis10BB and a related compound [15], suggest a possible mechanism—namely, that the presence throughout the nematic range of short-range correlated, tilted smectic clusters of bent-core molecules gives rise to additional SH scattering. The SAXS data indicate that the average director (molecular long axis) of these clusters is aligned by magnetic fields of ~ 1 T, that the cluster correlation lengths are of order a few layer spacings, and that the clusters are randomly distributed spatially. Moreover, they are observed in BCN samples that do not possess a lower temperature smectic phase, and differ in this respect from the pretransitional smectic "cybotactic" groups [33] characteristic of certain calamitics near a nematic to smectic-C transition. In the usual smectic-C phases of bent-core compounds the individual layers are polar (i.e., the molecules are packed with a common "bow" direction), and are stacked in either a ferroelectric (F) or antiferroelectric (AF) arrangement. Thus, we expect that smectic clusters in our BCN would have C_2 or D_2 point symmetry. Some recent reports provide evidence for both scenarios (and even suggest a transition between AF and F clusters in certain BCN compounds) [13,34]. In both instances, the clusters would be noncentrosymmetric, with the nonzero components of $\vec{\vec{\chi}}^{(2)}$ providing a potential source of SH signal distinct from the nonlinear scattering due to fluctuation-induced non-centrosymmetry in conventional nematics.

Given this basis for enhanced SHG in a BCN, one must explain the facts that the SH intensity is still rather weak, the presence of the node in forward transmission, and the features in the scattering in Fig. 5 occurring over optical wavevectors, which suggest a length scale within the sample considerably larger than the smectic cluster size indicated by SAXS. Starting with the latter issue, we suggest that the BCN is inhomogeneous: namely, that the sample contains either smectic clusters coexisting metastably with a simple nematic fluid, or a mixture of different smectic-C cluster types, distinguished by the syn/anticlinicity and/or ferro/antiferroelectricity of the smectic layering. This behavior is in fact frequently observed in bent-core smectics, where majority and minority domains of different layering variants comprise a "conglomerate" phase [35]. Either scenario could result in distinct domains in a BCN that are substantially larger than the individual smectic cluster size. Indeed, in "conglomerate" smectics, minority domains have been resolved in electro-optical studies [35].

Moreover, it is possible that within these domains in a BCN, orientational averaging in the plane perpendicular to the alignment direction $\hat{H}$ reduces the net second order dipole moment $\vec{p}_{eff}^{(2)}$ (a result that can be demonstrated for either D_2 or C_2 clusters, with the polarization in the C_2 case perpendicular to $\hat{H}$, as long as the clusters are small compared to the optical wavelength and randomly oriented in directions normal to $\hat{H}$), while the surfaces of the domains, spanning lengths comparable to λ, yield a more significant SH signal via the final term in Eq. (1) [36]. In this case of interfacial SHG, the node in the forward direction can also be explained. Experiments on colloidal particles [37,38],

with SH active surfaces but no contributing interior (or "bulk") $\vec{\vec{\chi}}^{(2)}$, show both a minimum SH signal in forward transmission and, for particle sizes ~100 nm, a pattern of SH scattering which, when integrated over our collection aperture, is rather similar to our observations in Fig. 5 [39]. To test the speculations we have made here, additional experiments on SH scattering from BCNs spanning a wider range of angles and under applied electric fields (or perhaps recorded immediately after rapid removal of an *E*-field) could be quite useful.

V. CONCLUSION

We have observed incoherent second-harmonic light scattering in the aligned nematic phase of a bent-core liquid crystal, and compared its properties to those observed for an ordinary calamitic liquid crystal. Our results for the latter can be adequately described by a theory of scattered SH light based on flexoelectric polarization induced by conventional director fluctuations, as originally studied by Copic and Ovsenik [4] and elaborated upon in the present work, both in terms of explicit features of the model and the range of experimental data compared to the theoretical predictions. However, this model does not account for key results observed in the bent-core nematic, particularly the angular dependence of the scattered SH power indicated by measurements over different collection solid angles. An intriguing scenario to explain this behavior is the nonlinear scattering arising from a spatial distribution of nanoscale tilted smectic molecular clusters, whose persistence through the nematic range has been confirmed in recent experimental studies on various bent-core compounds.

ACKNOWLEDGMENTS

This work was supported by NSF Grant No. DMR-0606160. The authors would like to acknowledge useful conversations with Professor D. Allender and Professor M. Copic.

[1] R. B. Meyer, Phys. Rev. Lett. **22**, 918 (1969).
[2] Y. R. Shen, Annu. Rev. Phys. Chem. **40**, 327 (1989); J. W. Shelton and Y. R. Shen, Phys. Rev. A **5**, 1867 (1972).
[3] K. Shia, T. Kosa, P. Palffy-Muhoray, and Y. S. Kim, Mol. Cryst. Liq. Cryst. (Phila. Pa.) **299**, 73 (1997).
[4] M. Čopič and T. Ovsenik, EPL **24**, 93 (1993).
[5] B. R. Acharya, A. Primak, and S. Kumar, Phys. Rev. Lett. **92**, 145506 (2004).
[6] L. A. Madsen, T. J. Dingemans, M. Nakata, and E. T. Samulski, Phys. Rev. Lett. **92**, 145505 (2004).
[7] V. Prasad, S. W. Kang, K. A. Suresh, L. Joshi, Q. Wang, and S. Kumar, J. Am. Chem. Soc. **127**, 17224 (2005).
[8] T. C. Lubensky and L. Radzihovsky, Phys. Rev. E **66**, 031704 (2002).
[9] K. Fodor-Csorba, A. Vajda, G. Galli, A. Jákli, D. Demus, S. Holly, and E. Gács-Baitz, Macromol. Chem. Phys. **203**, 1556 (2002).
[10] J. Harden, B. Mbanga, N. Eber, K. Fodor-Csorba, S. Sprunt, J. T. Gleeson, and A. Jakli, Phys. Rev. Lett. **97**, 157802 (2006).
[11] S. Stojadinovic, A. Adorjan, S. Sprunt, H. Sawade, and A. Jakli, Phys. Rev. E **66**, 060701 (2002).
[12] C. Bailey, Ph.D. dissertation, Kent State University, 2008.
[13] O. Francesangeli, V. Stanic, S. I. Torgova, A. Strigazzi, N. Scaramuzza, C. Ferrero, I. N. Dolbnya, T. M. Weiss, R. Berardi, L. Muccioli, S. Orlandi, and C. Zannoni, Adv. Funct. Mater. **19**, 2592 (2009).
[14] N. Vaupotič, J. Szydlowska, M. Salamonczyk, A. Kovarova, J. Svoboda, M. Osipov, D. Pociecha, and E. Gorecka, Phys. Rev. E **80**, 030701 (2009).
[15] S. Hong, R. Verduzco, J. Williams, R. Twieg, E. DiMasi, R. Pindak, A. Jakli, J. T. Gleeson, and S. Sprunt, Soft Matter **6**, 4819 (2010).
[16] No significant absorption at 1064 nm was recorded on a laboratory spectrophotometer for either of the liquid crystal compounds studied.
[17] R. W. Terhune, P. D. Maker, and C. M. Savage, Phys. Rev. Lett. **14**, 681 (1965).
[18] J. Zyss and I. Ledoux, Chem. Rev. **94**, 77 (1994).
[19] Gaussian03, Gaussian Inc. (2006).
[20] F. Araoka, B. Park, Y. Kinoshita, K. Ishikawa, H. Takezoe, J. Thisayukta, and J. Watanabe, Jpn. J. Appl. Phys., Part 1 **38**, 3526 (1999).
[21] J. E. Bjorkholm and A. E. Siegman, Phys. Rev. **154**, 851 (1967).
[22] Y. R. Shen, *The Principles of Nonlinear Optics*, Wiley Classics (Wiley, New York, 2003).
[23] J. I. Dadap, J. Shan, K. B. Eisenthal, and T. F. Heinz, Phys. Rev. Lett. **83**, 4045 (1999); J. I. Dadap, J. Shan, and T. F. Heinz, J. Opt. Soc. Am. B **21**, 1328 (2004); J. I. Dadap, Phys. Rev. B **78**, 205322 (2008).
[24] Ou-Yang Zhong-can and Xie Yu-zhang, Phys. Rev. A **32**, 1189 (1985).
[25] N. Bloembergen, R. K. Chang, S. S. Jha, and C. H. Lee, Phys. Rev. **174**, 813 (1968).
[26] P. G. deGennes and J. Prost, *The Physics of Liquid Crystals*, 2nd ed. (Clarendon Press, Oxford, 1993).
[27] See, e.g., P. N. Butcher and D. Cotter, *The Elements of Nonlinear Optics* (Cambridge University Press, Cambridge, England, 1991), Chap. 5.
[28] When transforming from scattering angle in the sample to the lab, the refractive index anisotropy Δn associated with a uniaxial medium will introduce corrections of higher order in $\sin\theta$ to the calculation of the dependence of $P^{(2)}$ on θ. However, these are small (proportional to powers of $\Delta n/\bar{n} \sim 0.1$) and so should not alter the basic conclusion.
[29] D. W. Allender, IMID Digest **1**, 195 (2005).
[30] D. W. Berreman and S. Meiboom, Phys. Rev. A **30**, 1955 (1984).
[31] I. Dozov, P. Martinot-Lagarde, and G. Durand, J. Phys. (France) Lett. **44**, 817 (1983).

[32] M. Majumdar, P. Salamon, A. Jakli, J. T. Gleeson, and S. Sprunt (unpublished).
[33] A. deVries, Mol. Cryst. Liq. Cryst. **10**, 219 (1970).
[34] M. Nagaraj, Y. P. Panarin, U. Manna, J. K. Vij, C. Keith, and C. Tschierske, Appl. Phys. Lett. **96**, 011106 (2010).
[35] For a review, see D. M. Walba, in *Topics in Stereochemistry*, edited by M. M. Green, R. J. M. Nolte, and E. W. Meijer (Wiley, New York, 2003), Vol. 24.
[36] If the clusters have AF (D_2) symmetry, the polarization cancels over neighboring layers. The cluster interior may then produce a weak SH response, regardless of cluster orientation. See, e.g., the results for conventional calamitic AFLCs reported in T. Fujioka, K. Kajikawa, H. Takezoe, A. Fukuda, T. Kusumoto, and T. Hiyama, Jpn. J. Appl. Phys., Part 1 **32**, 4589 (1993).
[37] J. Shan, J. I. Dadap, I. Stiopkin, G. A. Reider, and T. F. Heinz, Phys. Rev. A **73**, 023819 (2006).
[38] S.-H. Jen and H.-L. Dai, J. Phys. Chem. B **110**, 23000 (2006).
[39] N. Yang, W. E. Angerer, and A. G. Yodh, Phys. Rev. Lett. **87**, 103902 (2001).